Static and dynamic susceptibility of a mixed-valence impurity. II

P. Schlottmann
Fachbereich Physik, Freie Universität Berlin, Arnimallee 14, D-1000 Berlin 33, West Germany
(Received 5 July 1983)

We have calculated the static and dynamic susceptibility of mixed-valence impurities in a metallic host. We use a simple model consisting of two stable multiplets with angular momenta J_1 and J_2, that correspond to the $4f^{n+1}$ and $4f^n$ configurations, respectively, which are hybridized through the conduction-electron states. Two methods of calculation have been employed. For the static quantities we used an equation-of-motion method in connection with the fluctuation-dissipation theorem and the Brillouin-Wigner approach. The dynamic susceptibility is expressed in terms of a relaxation function $N(z)$, which is calculated within a mode-mode coupling approach and within the Brillouin-Wigner method. The results obtained by the different methods are compared and applied to the cases of Ce, Nd, and Tm impurities.

I. INTRODUCTION

Homogeneous intermediate-valence systems[1-3] are characterized by the quantum-mechanical superposition of two configurations of the highly correlated f states of the rare-earth-metal ions. Many of the unusual properties of these systems are caused by the competing effects of three types of energies: (a) the strong electron-electron repulsion in the f shell, (b) the delocalization of the conduction electrons, and (c) the hybridization mixing the f and conduction-band states.

Intermediate-valence impurities are usually described in terms of Anderson's model.[4] We consider only the Hund's rule ground multiplets of two ionic configurations, $4f^{n+1}$ and $4f^n$, and denote with J_1 and J_2 their total angular momenta, respectively. The two multiplets are mixed by a hybridization matrix element V. The hybridization induces f-charge fluctuations, which are accompanied by spin fluctuations. These charge and spin fluctuations determine the dynamics of the f electrons, which, complemented by the partition function, give a complete description of the mixed-valence impurity problem.

Several methods have been used to obtain the thermodynamics of a mixed-valence impurity. The possibly most successful one has been the Brillouin-Wigner approach,[5-8] but also the renormalization-group approach leads to similar results,[9,10] as well as the equation-of-motion method[11] in combination with the fluctuation-dissipation theorem. All these perturbation approaches converge and yield very similar results if $|J_1-J_2|$ is large and $\min(J_1,J_2)$ is small. They are based on the fact that the hybridization is a small energy parameter and that it can be treated as a perturbation.

The dynamic magnetic susceptibility, i.e., the f-electron relaxation rate, has been discussed in second order in the hybridization by several authors.[12-15] These results are valid only for temperatures much higher than the resonance width. Furthermore the energy shifts of the impurity levels, which stabilize the perturbation series,[6-9] only enter in higher order in V than the second. By using a mode-mode coupling approach within Mori's technique we have included the energy shifts and extended the range of validity of these results to all temperatures[11] (to be referred to as paper I). This approach has been successfully applied previously to the Kondo problem.[16,17]

At the Valence-Instability Conference in Zürich[3,18] we presented a different scheme, related to the Brillouin-Wigner method, to evaluate Mori's memory kernels. It is the purpose of this paper to discuss the latter approach in more detail and to compare the results of the two methods. We focus our attention especially on Ce, Tm, and Nd impurities in view of the numerous experimental results for the statics and the dynamics of these ions. The time-differential perturbed angular γ-ray distribution method of implanted rare-earth ions, used by Riegel *et al.*[19-21] yields, in principle, simultaneously the static spin susceptibility and the spin-relaxation rate. The neutron scattering spectrum measures the frequency dependence of the dynamic spin susceptibility. For TmSe and dilute mixed-valence Tm systems[22,23] an inelastic resonance has been found in addition to the usual quasielastic peak. The inelastic peak can be explained either by crystal-field splitting or by a coherent charge excitation.[24]

The rest of the paper is organized as follows. In Sec. II the model is described and some of its general properties are discussed. The dynamic susceptibilities are expressed in terms of relaxation functions by using Mori's method.[25-27] In Sec. III the mode-mode coupling approach is briefly summarized and extended to our model. The thermodynamics as given by the equation-of-motion method is discussed in the Appendix. In Sec. IV we present the details of the Brillouin-Wigner method to calculate the relaxation kernel of the dynamic susceptibilities. A comparison of the methods and a brief discussion of properties of Ce, Tm, and Nd impurities is given in Sec. V. A summary and the concluding remarks follow in Sec. VI.

II. MODEL AND FORMULAS

A. Model

Owing to the large electron-electron repulsion in the f shell only two ionic configurations, $4f^{n+1}$ and $4f^n$, are to

be considered. We employ Hund's rules to find the ground multiplets of these configurations and denote with J_1 and J_2, respectively, their total angular momenta, and with $E_{J_1M_1}$ and $E_{J_2M_2}$ we denote their energies. All other states except these multiplets are going to be neglected. The hybridization V of the f states with the conduction electrons induces charge fluctuations in the f-electron occupation and mixes the two configurations. The conduction-electron states are expanded in partial waves at the impurity site and only the states with total angular momentum $j=\frac{5}{2}$ and $\frac{7}{2}$ can contribute to the hybridization with f electrons. We are going to consider only one of these two partial waves and neglect the other one. For light rare-earth impurities that $j=\frac{5}{2}$ partial wave is the more important one and for heavy rare-earth ions we keep only the $j=\frac{7}{2}$ states. This simplification corresponds to a particular jj coupling instead of the usual Russell-Saunders coupling scheme. Instead of $9j$ symbols the Hamiltonian now just involves simple Clebsch-Gordan coefficients. In the case of Ce or Yb it does not represent an approximation. The Hamiltonian[18,28,29] may then be written $H=H_0+H_v$, where

$$\begin{aligned} H_0&=\sum_{\vec{k},m}\epsilon_k c^{\dagger}_{\vec{k}m}c_{\vec{k}m}+\sum_{M_1}E_{J_1M_1}B_{J_1M_1}+\sum_{M_2}E_{J_2M_2}B_{J_2M_2}\,,\\ H_v&=V(2J_2+1)^{1/2}\\ &\quad\times\sum_{\vec{k},m,M_1,M_2}(J_2M_2jm\,|\,J_2jJ_1M_1)\\ &\qquad\times(A^{\dagger}_{M_1M_2}c_{\vec{k}m}+c^{\dagger}_{\vec{k}m}A_{M_1M_2})\,. \end{aligned} \tag{2.1}$$

Here $c_{\vec{k}m}$ denotes the annihilation of a conduction electron with momentum $\vec{k}$, angular momentum j, and z component m. The Clebsch-Gordan coefficient selects $m=M_1-M_2$ (conservation of angular momentum). The operators B_{JM} and $A_{M_1M_2}$ are number operators and a charge-transfer operator, respectively, most conveniently expressed in terms of bras and kets,

$$\begin{aligned} A^{\dagger}_{M_1M_2}&=|J_1M_1\rangle\langle J_2M_2|\,,\\ B_{J_1M_1}&=|J_1M_1\rangle\langle J_1M_1|\,,\\ B_{J_2M_2}&=|J_2M_2\rangle\langle J_2M_2|\,. \end{aligned} \tag{2.2}$$

This model corresponds to the $U\to\infty$ limit of an Anderson impurity, which excludes states other than the J_1 manifold of the $4f^{n+1}$ and the J_2 manifold of the $4f^n$ configuration.

We will use the following shorthand notation for the Clebsch-Gordan coefficients:

$$(J_2M_2jm\,|\,J_2jJ_1M_1)\equiv(M_2m\,|\,M_1)\,, \tag{2.3}$$

and $|J_1M_1\rangle\equiv|M_1\rangle, |J_2M_2\rangle\equiv|M_2\rangle$ for the ionic states.

The ground-state properties of (2.1) for $J_2=0$ or $J_1=0$ have been exactly obtained by means of Bethe's ansatz.[30,31] In this case the ground state is a singlet. The case $J_2=0$ and $J_1=j=\frac{5}{2}$ corresponds to Ce impurities, $J_1=0$ and $J_2=j=\frac{7}{2}$ to Yb impurities; for Tm impurities we have $J_2=6$ and $J_1=j=\frac{7}{2}$, and for Nd impurities, $J_1=\frac{9}{2}$, $J_2=4$, and $j=\frac{5}{2}$.

B. General formulas

In this section we summarize the essential definitions and equations we need to calculate the dynamics of the impurity. We first give the general equations of Mori's formalism[25–27] and specialize them then to the dynamic susceptibilities.

Consider the space of operators built up by all possible products of f-electron operators and creation and annihilation operators of conduction electrons. We denote with (A,B) a scalar product defined onto this space, where A and B are two arbitrary vectors of the Hilbert space. Operators on this Hilbert space are denoted by script letters, e.g., the Liouville operator $\mathscr{H}$, defined by $\mathscr{H}A=(H,A)$, the resolvent $\mathscr{R}(z)=(z-\mathscr{H})^{-1}$, and projectors $\mathscr{P}$ and $\mathscr{Q}$. Let $\{A_\alpha\}$ be the set of N operators that are relevant to the properties under discussion. Mori's projection technique[25–27] then yields the following expression for the resolvent matrix elements between these operators:

$$\hat{\phi}(z)=(z\hat{1}-\hat{\Omega}-\hat{M}(z))^{-1}\hat{\chi}^0\,, \tag{2.4}$$

where $\hat{1}$ is the $N\times N$ unit matrix,

$$\phi_{\alpha\beta}(z)=(A_\alpha,\mathscr{R}(z)A_\beta)\,, \tag{2.5}$$

$$\chi^0_{\alpha\beta}=(A_\alpha,A_\beta)\,, \tag{2.6}$$

$$\hat{\Omega}=\hat{\omega}(\hat{\chi}^0)^{-1}\quad\omega_{\alpha\beta}=(A_\alpha,\mathscr{H}A_\beta)\,, \tag{2.7}$$

$$\hat{M}(z)=\hat{m}(z)(\hat{\chi}^0)^{-1},\quad m_{\alpha\beta}(z)=(\mathscr{Q}\mathscr{H}A_\alpha,\mathscr{R}_{\mathscr{Q}}(z)\mathscr{Q}\mathscr{H}A_\beta)\,. \tag{2.8}$$

Here $\mathscr{Q}$ projects onto the subspace orthogonal to the set $\{A_\alpha\}$ and $\mathscr{R}_{\mathscr{Q}}(z)$ is the resolvent within this subspace $\mathscr{R}_{\mathscr{Q}}(z)=(z\mathscr{Q}-\mathscr{Q}\mathscr{H}\mathscr{Q})^{-1}$. Note that $\hat{m}(z)$ is just a resolvent matrix element on the reduced subspace. Equations (2.4)–(2.8) can successively by applied and a continued fraction is generated in this way. $\hat{\Omega}$ and the real part of $\hat{M}(z)$ play the role of restoring forces, while the imaginary part of $\hat{M}(z)$ yields the lifetime. The many-body memory effects of $\hat{\phi}(z)$ are contained in $\hat{M}(z)$.

The success of the approach depends on (i) the appropriate choice of the set $\{A_\alpha\}$, (ii) a convenient choice of the scalar product (which is not unique), and (iii), since an exact evaluation of the memory functions is usually not possible, a physically meaningful decoupling of the continued fraction.

The relevant operator for the charge susceptibility is the f charge which may be defined as

$$q=\sum_{M_1}B_{J_1M_1}=1-\sum_{M_2}B_{J_2M_2}\,. \tag{2.9}$$

Note that since the impurity is always either in a $|J_1M_1\rangle$ state or in a $|J_2M_2\rangle$ state, the sum of all B_{JM} is 1. The relevant operators for the spin susceptibility are the total angular momentum operators of the two multiplets,

$$S_{J_1}=\sum_{M_1} M_1 B_{J_1 M_1},\quad S_{J_2}=\sum_{M_2} M_2 B_{J_2 M_2}\ . \tag{2.10}$$

Hence, in the case of the charge susceptibility, Eqs. (2.4)–(2.8) are scalars, while for the spin susceptibility they are 2×2 matrices.

The most appropriate scalar product to calculate dynamic susceptibilities is the static susceptibility

$$(A,B)=\chi_{A^\dagger B}(z=0)=i\int_0^\infty dt\, e^{i0^\dagger t}\langle [A^\dagger(t),B]\rangle\ . \tag{2.11}$$

The dynamic susceptibility can then be expressed in terms of (2.4)–(2.8) as

$$\hat{\chi}(z)=[z\hat{1}-\hat{\Omega}-\hat{M}(z)]^{-1}[-\hat{\Omega}-\hat{M}(z)]\hat{\chi}^0\ . \tag{2.12}$$

We define charge- and spin-current operators as follows:

$$j_q=[H_v,q]=V(2J_2+1)^{1/2}\sum_{\vec{k},m,M_1,M_2}(M_2 m\,|\,M_1)(c^\dagger_{\vec{k}m}A_{M_1M_2}-A^\dagger_{M_1M_2}c_{\vec{k}m}) \tag{2.13}$$

$$j_{S_1}=[H_v,S_{J_1}]=V(2J_2+1)^{1/2}\sum_{\vec{k},m,M_1,M_2}M_1(M_2 m\,|\,M_1)(c^\dagger_{\vec{k}m}A_{M_1M_2}-A^\dagger_{M_1M_2}c_{\vec{k}m})\ , \tag{2.14}$$

and similarly j_{s_2}. From the definition of $\omega_{\alpha\beta}$, (2.7), it is easy to show that the operators q, S_{J_1}, and S_{J_2} are orthogonal to their currents, such that $\Omega_{\alpha\beta}=0$ for the charge and spin susceptibilities. In second-order approximation and also in the leading logarithmic-order diagram resummation the projectors $\mathcal{Q}$ can be neglected. In this way we get

$$m_q(z)=[j_q,\mathcal{R}_{\mathcal{Q}}(z)j_q]=-(2J_1+1)(2J_2+1)N(z)\ , \tag{2.15}$$

$$m_{s_1s_1}(z)=-\tfrac{1}{3}(2J_1+1)(2J_2+1)J_1(J_1+1)N(z)\ , \tag{2.16a}$$

$$m_{s_2s_2}(z)=-\tfrac{1}{3}(2J_1+1)(2J_2+1)J_2(J_2+1)N(z)\ , \tag{2.16b}$$

$$m_{s_1s_2}(z)=m_{s_2s_1}(z)=\tfrac{1}{6}(2J_1+1)(2J_2+1)[J_1(J_1+1)+J_2(J_2+1)-j(j+1)]N(z)\ , \tag{2.16c}$$

where $N(z)$ is a function given by

$$(2J_1+1)(2J_2+1)N(z)=-V^2(2J_2+1)\sum_{\vec{k},m,M_1,M_2}(M_2 m\,|\,M_1)^2 \times(\langle\langle c^\dagger_{\vec{k}m}A_{M_1M_2};A^\dagger_{M_1M_2}c_{\vec{k}m}\rangle\rangle_z+\langle\langle A^\dagger_{M_1M_2}c_{\vec{k}m};c^\dagger_{\vec{k}m}A_{M_1M_2}\rangle\rangle_z)/z\ . \tag{2.17}$$

Here we neglected terms that are not of leading order.

Herewith we have expressed the dynamic susceptibilities in terms of the static quantities and the relaxation kernel $N(z)$. The function $N(z)$ and the static quantities are evaluated in Sec. III by using a mode-mode coupling approach[11] and in Sec. IV by means of a Brillouin-Wigner resummation. It is also interesting to note that the resistivity due to the impurity is also given by the function $N(z)$,

$$\rho=c\frac{k_F^2}{3N_e e^2}(2J_1+1)(2J_2+1)N''(0)\ , \tag{2.18}$$

where c is the impurity concentration, N_e is the number of electrons, and e is its charge. All relations are derived in the absence of an external magnetic field. The above relations have been obtained previously by Kuramoto and Müller-Hartmann[15] in second order in V for a more general model.

III. MODE-MODE COUPLING APPROACH FOR THE RELAXATION KERNEL

In Ref. 11 we have evaluated the relaxation function $N(z)$ for $J_2=0$ using the mode-mode coupling approach, and we will just sketch the method and state the results in the general case.

Within the noninteracting system the imaginary part of $N(z)$ can be factorized and one obtains

$$N''(\omega)=-\frac{\Gamma}{\omega}\int\frac{d\omega'}{2\pi}\left[\tanh\frac{\omega'}{2T}+\tanh\frac{\omega-\omega'}{2T}\right]\times[G_f''(\omega')+G_f''(-\omega')]\ , \tag{3.1}$$

where $\Gamma=\pi\rho V^2$ and $G_f(z)$ is the f-electron propagator defined as

$$G_f(z)=\langle\langle A_{M_1M_2};A^\dagger_{M_1M_2}\rangle\rangle_z\ . \tag{3.2}$$

We assume that $G_f(z)$ can be cast into the following form:

$$G_f(z)=\frac{\langle B_{J_1}\rangle+\langle B_{J_2}\rangle}{z-E_{J_1}+E_{J_2}-\tilde{\omega}_{J_1}+\tilde{\omega}_{J_2}-\Sigma(z)}\ , \tag{3.3}$$

where $\langle B_J\rangle$ are the occupation numbers of the f levels, $\tilde{\omega}_J$ are the energy shifts, and $\Sigma(z)$ is the f-level self-energy. Inserting G_f for $V\to 0$ into (3.1) we obtain

$$N''(0)=(\langle B_{J_1}\rangle+\langle B_{J_2}\rangle)\frac{\Gamma}{2T}\cosh^{-2}\left[\frac{E_{J_1}-E_{J_2}}{2T}\right], \quad (3.4)$$

which vanishes exponentially as $T\to 0$, unless accidentally $E_{J_1}=E_{J_2}$. A vanishing $N''(0)$ leads in general to a vanishing relaxation rate.

Higher-order contributions in V must be considered. A practicable scheme to include them partially is the mode-mode coupling approach. A similar approach has been successfully applied to the Kondo problem.[16,17]

Equation (3.1) may be interpreted as the bubble diagram shown in Fig. 1. A B_J correlation function decays into an f mode and a conduction-electron mode. The vertex is the hybridization V. The conduction-electron propagator is not substantially modified by the presence of one impurity. The f electron, on the other hand, has a high probability to decay into the conduction band due to the hybridization. The finite lifetime of the f electron is taken into account by the self-energy Σ in (3.3). In second order in V we have

$$\Sigma(z)=-i\Gamma/(\langle B_{J_1}\rangle+\langle B_{J_2}\rangle), \quad (3.5)$$

and the energy shifts $\tilde{\omega}_{J_1}$ and $\tilde{\omega}_{J_2}$ are evaluated consistently in leading logarithmic order,[32]

$$\tilde{\omega}_{J_1}=-(2J_2+1)\frac{\Gamma}{\pi}\left[\ln\frac{D}{2\pi T}-\mathrm{Re}\psi\left[\frac{1}{2}+\frac{\Gamma^*}{2\pi T}+i\frac{\Delta E}{2\pi T}\right]\right], \quad (3.6)$$

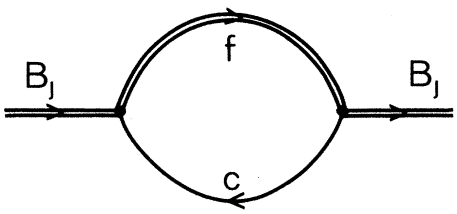

FIG. 1. Bubble diagram showing the decay of a B_J operator into a f propagator and a conduction electron. Double lines represent dressed propagators.

where ψ indicates a digamma function, and

$$\Delta E=E_{J_1}+\tilde{\omega}_{J_1}-E_{J_2}-\tilde{\omega}_{J_2}, \quad (3.7)$$

$$\Gamma^*=\frac{\Gamma}{\langle B_{J_1}\rangle+\langle B_{J_2}\rangle}, \quad (3.8)$$

and

$$(2J_2+1)\tilde{\omega}_{J_2}=(2J_1+1)\tilde{\omega}_{J_1}. \quad (3.9)$$

We do not consider vertex corrections in view of the renormalization-group result that Γ is not renormalized in the leading logarithmic approximation.[9]

Within this approximation the memory function $N(z)$ becomes

$$N(z)=\frac{\Gamma}{\pi z}(\langle B_{J_1}\rangle+\langle B_{J_2}\rangle)\left[2\,\mathrm{Re}\psi\left[\frac{1}{2}+\frac{\Gamma^*}{2\pi T}-i\frac{\Delta E}{2\pi T}\right]-\psi\left[\frac{1}{2}+\frac{\Gamma^*}{2\pi T}-i\frac{z+\Delta E}{2\pi T}\right]-\psi\left[\frac{1}{2}+\frac{\Gamma^*}{2\pi T}-i\frac{z-\Delta E}{2\pi T}\right]\right], \quad (3.10)$$

and the occupation numbers are given by

$$\frac{\langle B_{J_2}\rangle-\langle B_{J_1}\rangle}{\langle B_{J_2}\rangle+\langle B_{J_1}\rangle}=\frac{2}{\pi}\mathrm{Im}\psi\left[\frac{1}{2}+\frac{\Gamma^*}{2\pi T}+i\frac{\Delta E}{2\pi T}\right]. \quad (3.11)$$

The charge susceptibility is obtained by differentiating $\langle B_J\rangle$ with respect to $E_{J_1}-E_{J_2}$. The static spin susceptibility is discussed in the Appendix.

This is the generalization of the results of Ref. 11 to the model (2.1). The equations are valid in the absence of a magnetic field. Expression (3.10) is an overestimation of the relaxation rate, since we neglected the vertex corrections which partially compensate the self-energy effects.

IV. BRILLOUIN-WIGNER METHOD

In this section we calculate the memory function $N(z)$ by using a method that is related to the Brillouin-Wigner resummation technique.[7] The results of this section have been presented at the Zürich Conference.[3,18] We present here the details of the calculation.

A Brillouin-Wigner resummation of the perturbation series can be performed in two ways: (a) diagrammatically,[7] or (b) by equations of motion.[28] The latter way only involves traces over operators and two commutators with the interaction Hamiltonian for each logarithmic order, i.e., one commutator with H_v in leading order, three commutators in next-leading order, etc. We use this latter way.

The $[(2J_1+1)+(2J_2+1)]$ f states are mutually excluding, i.e., only one can be occupied at a time, and do not obey Fermi statistics. This is the consequence of the high correlations between the f electrons. It is then convenient to separate explicitly these states in the trace of the thermal averages,

$$\langle X\rangle=\sum_{M_1}\langle X\rangle_{J_1M_1}+\sum_{M_2}\langle X\rangle_{J_2M_2}, \quad (4.1)$$

where $\langle\ \rangle_{JM}$ denotes the trace over matrix elements with the ion in the $|JM\rangle$ f state. The Boltzmann factor $\exp(-\beta H)$ is included in the trace. We now define the operation[28]

$$(A,B)_{JM}=\langle A^\dagger B\rangle_{JM}=\mathrm{Tr}_{JM}(A^\dagger B e^{-\beta H}), \quad (4.2)$$

which has the following properties: (i) It is conjugate bilinear, (ii) $(A,A)_{JM}\geq 0$, positive definite, (iii) $(A,A)_{JM}=0$ if and only if $A=0$ or $A^\dagger$ has no matrix elements with fi-

nal state $|JM\rangle$, and (iv) it is Hermitian nonsymmetric, i.e., it is, in general, $(A,A)_{JM} \neq (A^\dagger, A^\dagger)_{JM}$. Since the operation (4.2) is not Hermitian symmetric, it is not an ordinary scalar product and our operator space is not a Hilbert space.

In Sec. II B we argued that Mori's formalism is defined on a Hilbert space. The Hermitian symmetry of the scalar product is, however, not necessary for the validity of (2.4)–(2.8). One has to distinguish among projectors from the right and left, which are, in general, not the same. A more detailed discussion of Mori's method defined on the operation (4.2) can be found in Ref. 28.

We evaluate the absorption and emission parts of a correlation function separately and write

$$\langle\langle c^\dagger_{\vec{k}m} A_{M_1M_2}; A^\dagger_{M_1M_2} c_{\vec{k}m} \rangle\rangle_z = \left\langle c^\dagger_{\vec{k}m} A_{M_1M_2} \frac{1}{z-\mathscr{H}} A^\dagger_{M_1M_2} c_{\vec{k}m} \right\rangle - \left\langle A^\dagger_{M_1M_2} c_{\vec{k}m} \frac{1}{z+\mathscr{H}} c^\dagger_{\vec{k}m} A_{M_1M_2} \right\rangle . \tag{4.3}$$

The thermal averages in (4.3) are separated in partial traces according to (4.1). Only two terms contribute in the leading-order approximation (the other traces vanish),

$$\left\langle c^\dagger_{\vec{k}m} A_{M_1M_2} \frac{1}{z-\mathscr{H}} A^\dagger_{M_1M_2} c_{\vec{k}m} \right\rangle_{J_2M_2} - \left\langle A^\dagger_{M_1M_2} c_{\vec{k}m} \frac{1}{z+\mathscr{H}} c^\dagger_{\vec{k}m} A_{M_1M_2} \right\rangle_{J_1M_1} . \tag{4.4}$$

According to (2.5)–(2.8) the first term of (4.4) can be written as

$$\frac{f(\epsilon_k)\langle B_{J_2}\rangle}{z+\epsilon_k - E_{J_1} + E_{J_2} + \omega_{J_2} + M_{kJ_2}(z)} , \tag{4.5}$$

where

$$\omega_{J_2}\langle B_{J_2}\rangle = V(2J_2+1)^{1/2} \sum_{\vec{p},m',M_1'} (M_2 m' \,|\, M_1')\langle c^\dagger_{\vec{p}m'} A_{M_1'M_2}\rangle_{J_2M_2} , \tag{4.6}$$

and $M_{\vec{k}J_2}(z)$ is another resolvent matrix element within a reduced subspace of our operator space. In (4.6) we neglected nonleading higher-order corrections by assuming

$$\langle c^\dagger_{\vec{k}m} c_{\vec{k}m} c^\dagger_{\vec{p}m'} A_{M_1'M_2}\rangle_{J_2M_2} \sim f(\epsilon_k)\langle c^\dagger_{\vec{p}m'} A_{M_1'M_2}\rangle_{J_2M_2} . \tag{4.7}$$

The projectors in $M_{kJ_2}(z)$ do not contribute up to the next-leading logarithmic order and are neglected. Denoting

$$h_{\vec{k}M_1M_2} = V(2J_2+1)^{1/2} \times \sum_{\vec{p},m',M_1',M_2'} (M_2'm' \,|\, M_1')(\delta_{M_1M_1'} \,|\, J_2M_2'\rangle\langle J_2M_2 \,|\, c^\dagger_{\vec{p}m'} c_{\vec{k}m} - \delta_{M_2M_2'} \,|\, J_1M_1\rangle\langle J_1M_1' \,|\, c_{\vec{k}m} c^\dagger_{\vec{p}m'}) . \tag{4.8}$$

we then have that

$$f(\epsilon_k)\langle B_{J_2}\rangle M_{\vec{k}J_2}(z) \approx \left\langle h^\dagger_{\vec{k}M_1M_2} \frac{1}{z-\mathscr{H}} h_{\vec{k}M_1M_2} \right\rangle_{J_2M_2} . \tag{4.9}$$

In leading order, only states within the $|J_2M_2\rangle$ multiplet are relevant and we obtain

$$M_{\vec{k}J_2}(z) = -(2J_2+1)V^2 \sum_{\vec{p}} \frac{1-f(\epsilon_p)}{z+\epsilon_k-\epsilon_p+\omega_{J_2}+M_{\vec{k}pJ_2}(z)} , \tag{4.10}$$

where again a factorization of the type (4.7) has been used. $M_{\vec{k}pJ_2}(z)$ is again a resolvent matrix element in a reduced space. The procedure can be carried on and a continued fraction is generated.

Similarly, for the second term of (4.4), we have

$$\frac{[1-f(\epsilon_k)]\langle B_{J_1}\rangle}{z+\epsilon_k - E_{J_1} + E_{J_2} - \omega_{J_1} + M_{\vec{k}J_1}(z)} , \tag{4.11}$$

where ω_{J_1} is given by an expression similar to (4.6) and

$$M_{\vec{k}J_1}(z) = -(2J_1+1)V^2 \sum_{\vec{p}} \frac{f(\epsilon_p)}{z+\epsilon_k-\epsilon_p-\omega_{J_1}+M_{\vec{k}\vec{p}J_1}(z)} , \tag{4.12}$$

etc.

The analytic properties of these continued fractions are complex. Similar regularization problems were found by Keiter *et al.*[33] for the f propagator. Their regularization technique leads to an integral equation, which seems not yet solved. The solution of the integral equation would give the exact Green's function in the next-leading logarithmic approximation. We are going to use a less sophisticated scheme, which is only approximate but leads to tractable results.[18]

We consider the remainder in (4.12), which for $T \to 0$ can be approximated by

$$\begin{aligned} M_{\vec{k}pJ_1}(z) &\approx -(2J_2+1)V^2 \sum_q \frac{1-f(\epsilon_q)}{z+\epsilon_k-\epsilon_p+\epsilon_q-\Delta E} \\ &\simeq -(2J_2+1)\frac{\Gamma}{\pi}\ln\frac{D}{z+\epsilon_k-\epsilon_p-\Delta E} \\ &\approx \omega_{J_1} - (2J_2+1)\frac{\Gamma}{\pi}\ln\frac{|\Delta E|}{z+\epsilon_k-\epsilon_p-\Delta E} , \end{aligned} \tag{4.13}$$

where $\Delta E = E_{J_1} + \omega_{J_1} - E_{J_2} - \omega_{J_2}$. The Fermi functions in (4.11) and (4.12) require that $\epsilon_k > 0$ and $\epsilon_p < 0$. Hence the imaginary part of (4.13) vanishes if $\omega > \Delta E$. Let us analyze the denominator of (4.12) for $\omega > \Delta E$. We call $X = \omega + \epsilon_k - \epsilon_p$; then the real part vanishes if

$$X - (2J_2+1)\frac{\Gamma}{\pi}\ln\frac{|\Delta E|}{|X-\Delta E|} = 0 . \tag{4.14}$$

This equation is satisfied for $X=0$ and it has in addition two solutions that for small Γ are close to $X=\Delta E$. They are approximately given by

$$X_{\pm} \simeq \Delta E \pm \Delta E \exp\left[-\frac{\pi \Delta E}{(2J_2+1)\Gamma}\right] = \Delta E \pm \delta . \tag{4.15}$$

Consider $\Delta E + \delta > \omega > \Delta E$; then for the solutions $X=0$ and X_- there is always an integration region such that the imaginary part of $M_{\vec{k}\vec{p}J_1}(z)$ is nonzero. The solution X_+, however, lies outside the continuum of excitations. The denominator in (4.12) vanishes at X_+ and gives rise to a pole, which then contributes to the imaginary part of $M_{\vec{k}J_1}(z)$. Hence the imaginary part of $M_{\vec{k}J_1}(z)$ no longer vanishes in the interval $\delta > \omega - \Delta E$. Note that δ is essentially the Kondo temperature.

The above argument was for the third step of the continued fraction. A similar pole appears also in the fifth, the seventh, and, in general, in the $(2n+1)$th step of the continued fraction. This sequence of poles smears the step function (at $T=0$) at $\omega = \Delta E$. We roughly approximate $M_{\vec{k}J_1}(z)$ by

$$M_{\vec{k}J_1}(z) = \omega_{J_2} + (2J_1+1)\Gamma i , \tag{4.16}$$

which certainly overestimates the imaginary part, but is the simplest meaningful approximation.

The other continued fractions (4.15) and (4.10) have similar analytical behavior. Here we find the poles in the fourth, the sixth, and, in general, in the $(2n+2)$th step of the continued fraction. Similarly we approximate (4.10) by

$$M_{\vec{k}J_2}(z) = -\omega_{J_1} + (2J_2+1)\Gamma i , \tag{4.17}$$

and the crudeness of this expression is the same as (4.16).

The second correlation function in (2.17) that contributes to $N(z)$ is evaluated in the same way and has the poles close to $\omega = -\Delta E$.

The $\vec{k}$ integration in (2.17) is now straightforward and we obtain

$$N(\omega) = -\frac{\Gamma}{\pi}\langle B_{J_1}\rangle \left[2\,\mathrm{Re}\psi\left(\frac{1}{2} + \frac{(2J_1+1)\Gamma}{2\pi T} - i\frac{\Delta E}{2\pi T}\right) - \psi\left(\frac{1}{2} + \frac{(2J_1+1)\Gamma}{2\pi T} - i\frac{\omega + \Delta E}{2\pi T}\right) - \psi\left(\frac{1}{2} + \frac{(2J_1+1)\Gamma}{2\pi T} - i\frac{\omega - \Delta E}{2\pi T}\right)\right] \Big/ \omega + (J_2 \leftrightarrow J_1) . \tag{4.18}$$

This expression is similar to the corresponding one within the mode-mode coupling approach, Eq. (3.10). The origin of the Γ in the argument of the digamma functions is the finite linewidth of the f states, which is proportional to the corresponding degeneracies of the multiplets.

A physical interpretation of the poles is also possible. The continued fraction is constructed with infinitely lived f states (V is the perturbation) and at any finite step the structure of the Fermi functions is such that the continuum of excitations vanishes for $\omega > \Delta E$ for the first term in (2.17) and for $\omega < -\Delta E$ for the second term. The finite lifetime of the f states is then generated by nonanalytic terms, i.e., the poles, which smear the step behavior at $\omega = \pm \Delta E$.

The energy shifts ω_{JM} are given by the self-consistent set of equations[18]

$$\omega_{J_1M_1} = \frac{\Gamma}{\pi}\sum_{M_2}\left[\ln\frac{D}{2\pi T} - \mathrm{Re}\psi\left(\frac{1}{2} - i\frac{\Delta E_{M_1M_2}}{2\pi T}\right)\right] , \tag{4.19}$$

and similarly $\omega_{J_2M_2}$, where

$$E_{M_1M_2} = E_{J_1M_1} - E_{J_2M_2} + \omega_{J_1M_1} - \omega_{J_2M_2} .$$

The partition function and hence the thermodynamics is obtained from

$$Z = \sum_{M_1}\exp[-\beta(E_{J_1M_1} + \omega_{J_1M_1})] + \sum_{M_2}\exp[-\beta(E_{J_2M_2} + \omega_{J_2M_2})] . \tag{4.20}$$

Equations (4.19) and (4.20) are valid in the presence of a magnetic field; all other equations hold for zero-field only. Equation (4.19) is a simplified version of the next-leading Brillouin-Wigner approximation.[5-7] In the leading-order approximation $\Delta E_{M_1M_2}$ in (4.19) is to be replaced by $E_{J_1M_1} + \omega_{J_1M_1} - E_{J_2M_2}$. The exact next-leading-order energy shifts are considerably more complicated.[5,7] The approximation is consistent within the logarithmic hierarchy, since (4.19) includes all the $\ln D$ dependences up to that order. Equations (4.19) and (4.20) form precisely the renormalization-group result within the leading logarithmic approximation.[9] The matrix susceptibility is obtained by differentiating (4.20) two times with respect to the Zeeman energies of the multiplets.

V. RESULTS

In this section we compare the mode-mode coupling results with those of the Brillouin-Wigner resummation and apply them to the case of Ce, Tm, and Nd impurities.

A. Valence and static spin susceptibility

We first compare the static quantities as given by Eqs. (4.19) and (4.20) (simplified Brillouin-Wigner resummation) with those within the equation-of-motion method summarized in the Appendix. We refer specifically to the case of Ce, for which $J_1=j=\frac{5}{2}$, $J_2=0$, and $g_{J_1}=\frac{6}{7}$. We choose $D=100\pi\Gamma$ and denote $E=E_{J_1}-E_{J_2}$. The static spin susceptibility and the occupation of one J_1 level are shown for $E=0$ and $E=4\Gamma$ as a function of temperature in Figs. 2 and 3. The dashed-dotted line in Fig. 3 denotes the high-temperature asymptotics of $\langle B_{J_1}\rangle$. The solid lines are the results within the Brillouin-Wigner approach and the dashed curves correspond to the equation-of-motion method.

The results within both approaches are very similar and differ by at most 20%. This is the consequence of the good convergence of the perturbation series for large $|J_1-J_2|$ as pointed out by Ramakrishnan.[6] With increasing $|J_1-J_2|$ the energy difference ΔE grows and $\Gamma/\Delta E$ becomes a small parameter. The nonleading terms, which are picked up differently by the two approaches, are then not very relevant, such that any meaningful decoupling would give a reasonable result. Note that for $E=4\Gamma$ the energy difference ΔE is almost 2 times larger than for $E=0$.

The ground state is a singlet with a van Vleck admixture of the J_1 multiplet. The $T=0$ susceptibility is then finite. When the temperature is raised the occupation of the J_1 multiplet grows by thermal population. Hence the susceptibility also increases and approaches at high T the expected Curie law. At high T all levels are equally populated. The valence of a Ce impurity is given by $\nu=4-(2J_1+1)\langle B_{J_1}\rangle$.

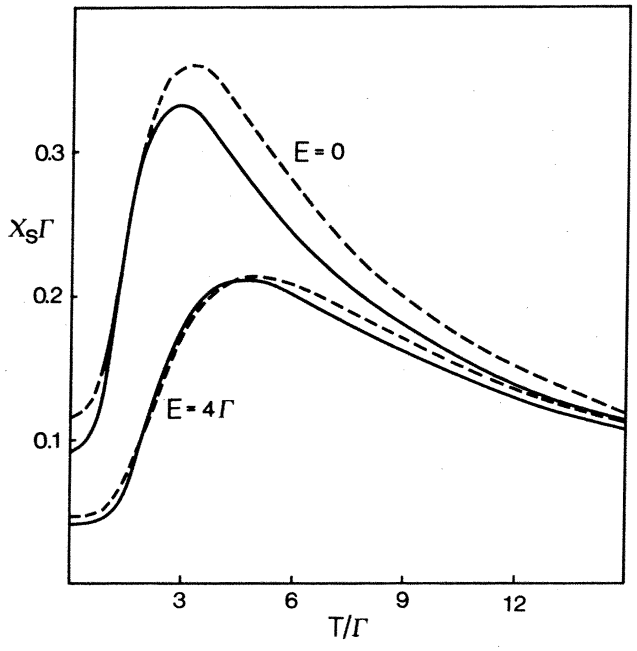

FIG. 2. Static spin susceptibility for Ce. The dashed lines are the results within the equation-of-motion method, Eqs. (A3)–(A6) of the Appendix, and the solid lines correspond to the Brillouin-Wigner method, Eqs. (4.19) and (4.20). The parameters are $J_1=j=\frac{5}{2}$, $J_2=0$, $g_{J_1}=\frac{6}{7}$, $D=100\Gamma\pi$, and $E=E_{J_1}-E_{J_2}$.

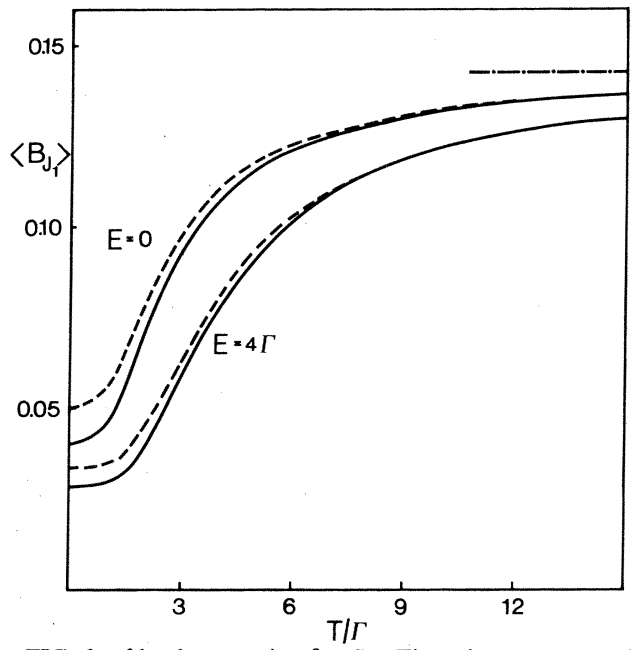

FIG. 3. f-level occupation for Ce. The valence corresponds to $4-6\langle B_{J_1}\rangle$. Parameters and notation as in Fig. 2.

B. Validity of the approximation

The exact ground-state properties of the model for $J_2=0$ and arbitrary $j=J_1$ have been obtained by means of Bethe's ansatz.[3] The spin susceptibility consists of two terms: a Kondo contribution and a mixed-valence contribution. The Kondo effect is not included in the approximations discussed in the present paper. The approximations are then valid if the Kondo part is much smaller than the mixed-valence contribution. This is the case for $n_f<0.3$ or $E>0$ for $J_1=\frac{5}{2}$. The range of validity is therefore considerably smaller than postulated by Ramakrishnan.[6]

C. Relaxation function

The imaginary part of the relaxation function $N(z)$ as given by the crudely approximated Brillouin-Wigner approach (solid line) and the mode-mode coupling method (dashed line) are shown for $T=0$ as a function of frequency in Fig. 4. Part (a) shows the case of Ce and part (b) shows the case of Tm. Once more the difference between the two methods is very small due to the good convergence of the perturbation theory, since $|J_1-J_2|=\frac{5}{2}$ for both cases.

The approaches always yield a finite $N''(\omega)$ for zero temperature and zero frequency. If ΔE is large enough, i.e., larger than the width of the levels E_{J_1} and E_{J_2} given by $(2J_2+1)\Gamma$ and $(2J_1+1)\Gamma$, respectively, a bump develops at $|\omega|\gtrsim\Delta E$. Its physical origin is that the external energy ω (provided by neutrons or photons) in-

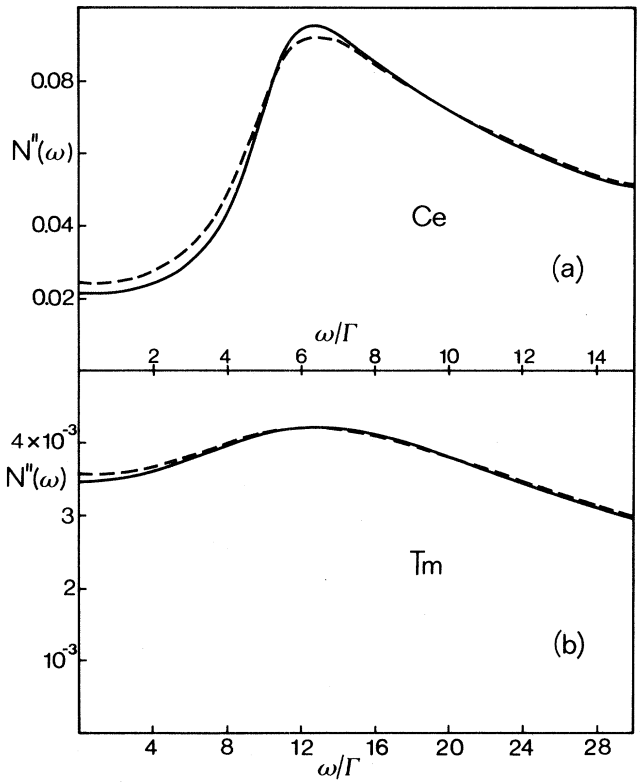

FIG. 4. Imaginary part of the memory function as a function of external frequency at zero temperature: (a) $J_1=j=\frac{5}{2}$, $J_2=0$, $\Delta E=5\Gamma$, and $\langle B_{J_1}\rangle=0.04$, and (b) for $J_1=6$, $J_2=j=\frac{7}{2}$, $\Delta E=10\Gamma$, and $\langle B_{J_1}\rangle=0.02$. The solid curves correspond to the crudely approximated Brillouin-Wigner method and the dashed lines correspond to the mode-mode coupling approach. $D=100\pi\Gamma$.

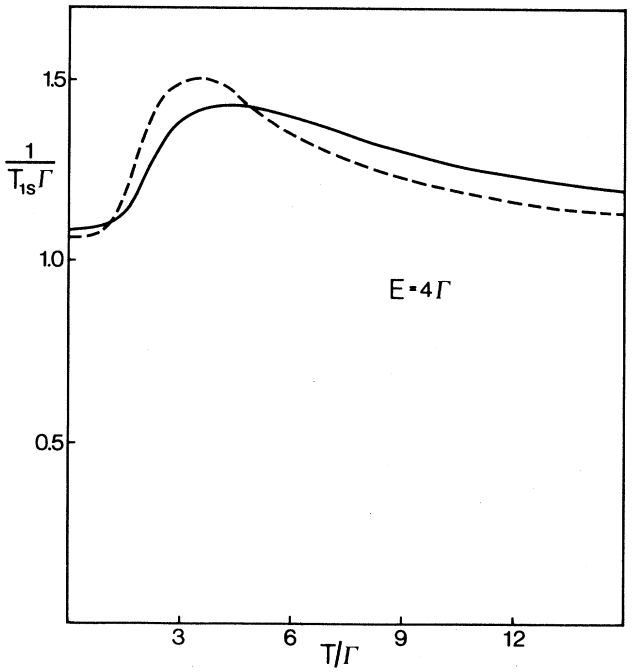

FIG. 5. Halfwidth of the quasielastic peak of the dynamic spin susceptibility (relaxation rate) for Ce impurities. The solid line is the simplified result within the Brillouin-Wigner approach and the dashed line is the simplified result within the mode-mode coupling method. The parameters are $J_1=j=\frac{5}{2}$, $J_2=0$, $E=4\Gamma$, $g_{J_1}=\frac{6}{7}$, and $D=100\pi\Gamma$.

duces transitions from the J_2 states to the J_1 levels (bonding and antibonding states). In the absence of an external energy the transition intensity is just given by the overlap of the Lorentzians associated with the J_1 and J_2 levels. If ΔE is large only the tails overlap and $N''(0)$ is small. The bump is the on-resonance condition for the transition. The bump disappears at higher temperatures since the thermal bath provides the energy for the transition.

The bump for Ce is considerably more pronounced than the one of Tm. This is the consequence of the larger degeneracies of the Tm levels. The levels are then rather broad and the Lorentzians strongly overlap already for zero frequency.

D. Dynamics of a mixed-valence Ce impurity

The main feature of the dynamic susceptibility of a Ce impurity is the quasielastic peak. It is caused by the spin-flip transitions within the J_1 multiplet, which are quasielastic in the absence of a magnetic field. The halfwidth of the quasielastic peak is the spin-relaxation rate shown in Fig. 5 as a function of temperature for $E=4\Gamma$. The solid line is the result within the simplified Brillouin-Wigner approach and the dashed line shows the mode-mode coupling result with the static quantities obtained within the equation-of-motion method.

Once more both methods yield similar results as a consequence of the good convergence of the perturbation expansion.[6] The relaxation rate is only weakly temperature dependent. It is enhanced for $T\simeq\Delta E$ since the J_1 multiplet becomes thermally populated. In other words, the thermal bath provides the energy for the transitions to the J_1 multiplet and accelerates the spin decay.

The dynamic susceptibility is drawn as a function of frequency in Fig. 6. Note that the area under the curves is normalized to 1. At high temperatures the shape is Lorentzian. At low T we have, in addition to the quasielastic peak, a bump for $|\omega|\gtrsim\Delta E$. This bump is the consequence of the inelastic peak in $N''(\omega)$ Its importance grows with increasing E. Note that the inelastic peak becomes a very large bump in a plot of $\chi_s''(\omega)$ instead of χ_s''/ω (see Fig. 3 of Ref. 18).

E. Susceptibility of a mixed-valence Tm impurity

Both configurations of a mixed-valence Tm impurity are magnetic. In order to be consistent with Refs. 18, 28, and 29 we choose $J_1=6$, $J_2=j=\frac{7}{2}$, $g_{J_1}=\frac{7}{6}$, and $g_{J_2}=\frac{8}{7}$. This corresponds to work with holes instead of electrons, but is otherwise equivalent to the Tm problem.

Since both configurations are magnetic, we define a susceptibility matrix $\hat{\chi}(z)$ according to (2.12) and obtain the actual susceptibility by multiplying with the corresponding Landé factors

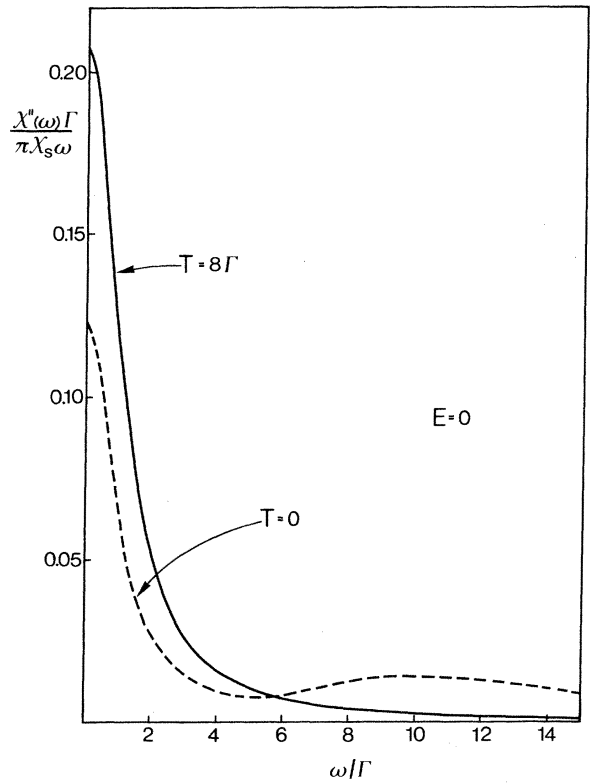

FIG. 6. Dynamic susceptibility of a Ce impurity as a function of frequency for two temperatures. At low T an inelastic peak develops at $|\omega| \gtrsim \Delta E$. Note that the area under the curves is normalized to 1. The parameters are $J_1=J=\frac{5}{2}$, $J_2=0$, $g_{J_1}=\frac{6}{7}$, $D=100\pi\Gamma$, and $E_{J_1}=E_{J_2}$. χ_s is the static spin susceptibility (Brillouin-Wigner approach).

$$\chi_s(z)=(g_{J_1}\ g_{J_2})\hat{\chi}_s(z)\begin{pmatrix} g_{J_1} \\ g_{J_2}\end{pmatrix}. \tag{5.1}$$

The static susceptibility essentially follows a Curie law. The Curie constant as obtained from the Brillouin-Wigner approximation is shown as a function of temperature in Fig. 7 for $E=10\Gamma$. The dashed line denotes the high-temperature asymptotics. The temperature dependence of the Curie constant is weak, and only at low T does it deviate considerably from the free-ion value.

Although the difference in angular momenta, $|J_1-J_2|$, is $\frac{5}{2}$ as for Ce impurities, the convergence of the perturbation series is less good for Tm than for Ce. A careful analysis of ω_{J_1} and ω_{J_2} and their field derivatives shows that the Ramakrishnan argument[6] is valid only if $|J_1-J_2|$ is large *and* if $\min(J_1,J_2)$ is small. The range of validity of the theory for Tm is roughly $E>4\Gamma$, while for Ce it is $E>0$ (see Sec. V B).

The dynamic susceptibility of Tm impurities shows a quasielastic peak. Its halfwidth is the spin-relaxation rate. Owing to the Curie law it follows a Korringa-type behavior at low T. The relaxation rate saturates at high temperatures since

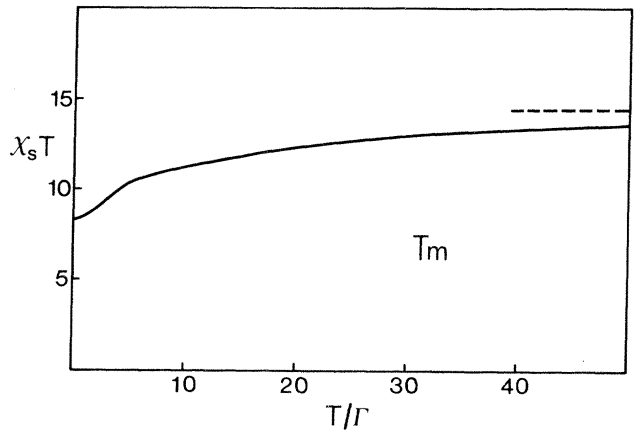

FIG. 7. Curie constant for a mixed-valence Tm impurity as a function of temperature (Brillouin-Wigner approach). The parameters are $J_1=6$, $J_2=j=\frac{7}{2}$, $g_{J_1}=\frac{7}{6}$, $g_{J_2}=\frac{8}{7}$, $D=100\pi\Gamma$, and $E=10\Gamma$. The dashed line is the high-temperature asymptotics.

$$N''(0)\sim\frac{1}{T}\ \text{at high } T\ , \tag{5.2}$$

as can be seen from the second-order perturbation, and $N''(0)$ compensates for the Curie law. (See Fig. 8.) This behavior of $1/T_{1s}$, Korringa at low T and constant at high T, has been observed[22] for the compound TmSe and recently also for diluted Tm alloys.[23]

The neutron scattering experiments[22,23] also revealed the existence of an inelastic peak, similar to the one discussed in Sec. V D. Our theory yields the inelastic peak for $\chi_s''(\omega)$ only for large ΔE, i.e., $\Delta E>(2J_1+2J_2+2)\Gamma$, as we explained in Sec. V C. The theory requires improvements in order to explain the inelastic peak in Tm as suggested by Mazzaferro *et al.*[24] This point is discussed with more detail in Sec. VI.

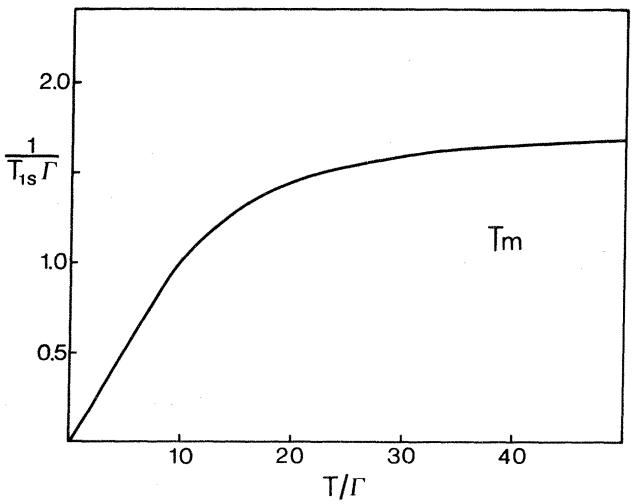

FIG. 8. Spin-relaxation rate (halfwidth of the quasielastic peak of the dynamic spin susceptibility for a Tm impurity as a function of temperature. The parameters are those of Fig. 7. At low T the linewidth follows a Korringa rate which saturates at high T.

F. Mixed-valence Nd impurities

The case of Nd ions is similar to Tm impurities in the sense that also here both configurations are expected to be magnetic: Nd^{3+} ($4f^3$) has $J_1=\frac{9}{2}$ and $g_{J_1}=\frac{8}{11}$, and the ground state of Nd^{4+} ($4f^2$) is $J_2=4$ and $g_{J_2}=\frac{4}{5}$. The theory for our model then yields similar results as for the Tm susceptibility as we show in Fig. 9. It is necessary here to choose a large E since $|J_1-J_2|$ is only 0.5.

The high-temperature static susceptibility of Nd impurities does not give information about the valence, since the ionic Curie constants of Nd^{3+} and Nd^{4+} are essentially the same. Our model yields a Curie law also for mixed-valence impurities even down to very low temperatures. Large deviations from such a behavior or even a saturation of the susceptibility at low T would be an indication that either of the crystal fields is important, i.e., larger than the f-level width, or that a more realistic model should be used (including fractional parentages). Perturbed angular γ-ray distribution measurements of the static impurity susceptibility of Nd ions in several hosts are presently carried out by Riegel *et al.*[21]

G. Resistivity and reduction of superconductor T_c

The resistivity and magnetoresistivity of mixed-valence Ce and Tm ions has been calculated by Foglio *et al.*[29]

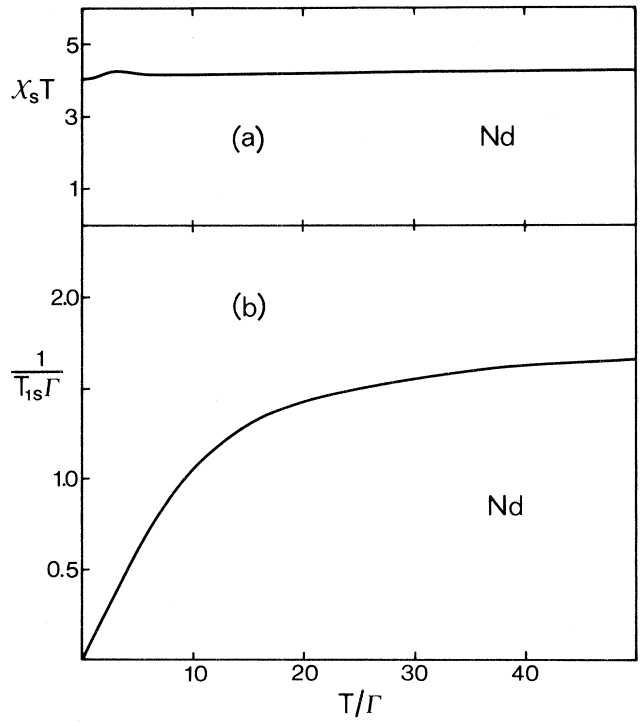

FIG. 9. (a) Curie constant and (b) spin-relaxation rate for a mixed-valence Nd impurity as a function of temperature (Brillouin-Wigner approach). The parameters are $J_1=\frac{9}{2}$, $J_2=4$, $j=\frac{5}{2}$, $g_{J_1}=\frac{8}{11}$, $g_{J_2}=0.8$, $D=100\pi\Gamma$, and $E=10\Gamma$. The Curie constant is essentially constant over the whole temperature range. The relaxation follows a Korringa law at low T and saturates at high T.

through Kubo's formula by making use of the procedure developed by Götze and Wölfle.[34] The zero-field resistivity is essentially given by (2.18). The method of calculation and the approximations involved are similar to the ones used in the present paper.

The reduction of T_c and other properties of a superconductor due to mixed-valence impurities can be found in Refs. 35 and 36. The method and the approximations are again the same ones employed here.

VI. CONCLUSIONS

We have calculated the static and dynamic susceptibilities of mixed-valence impurities in a metallic host using a simple model that consists of two *stable* multiplets of degeneracy $2J_1+1$ and $2J_2+1$, corresponding to the $4f^{n+1}$ and $4f^n$ configurations, respectively, which are hybridized through the conduction-electron states. The model is possibly the simplest impurity model that includes the orbital degeneracy of the f electrons. Two methods of calculation have been employed. For the static quantities we used an equation-of-motion method in connection with the fluctuation-dissipation theorem and a modified version of the Brillouin-Wigner resummation. The dynamic susceptibility has been expressed in terms of a relaxation kernel $N(z)$. This memory function has been calculated (a) by using a mode-mode coupling approach, and (b) within a continued-fraction resummation of the Brillouin-Wigner type.

We compared the results within the two methods for the static and dynamic quantities and we found that they differ only by the order of 10% within the range of validity of the approximations. This is the consequence of the good convergence of the perturbation expansion for large $|J_1-J_2|$ as pointed out by Ramakrishnan.[6] We found that the convergence does not only depend on $|J_1-J_2|$ but also on $\min(J_1,J_2)$. The convergence gets worse with growing $\min(J_1,J_2)$, i.e., the range of validity of the theory is reduced. Note that the range of validity is smaller than estimated by Ramakrishnan.

We would like to remark that previous theories by Balseiro and López,[12] Foglio,[13] and Kuramoto and Müller-Hartmann,[14,15] in which relaxation functions or self-energies were calculated up to second order in V, are recovered when we expand our results in powers of V. Note that the results of Ref. 12–15 are only valid for high temperatures.

We applied our results to the cases of mixed-valence Ce, Tm, and Nd ions. The model yields a singlet ground state if either J_1 or J_2 are zero. Otherwise the ground state is magnetic and we obtain a Curie-type susceptibility. The static susceptibility for "singlet ions," e.g., Ce and Yb, is finite at low T, grows then when the temperature is raised, and approaches a Curie law at high T.

The dynamic susceptibility has two main features: a quasielastic peak at $\omega=0$ and inelastic peaks at $|\omega| \gtrsim \Delta E$. The width of the quasielastic peak is only weakly temperature dependent for the singlet ions, in agreement with experimental neutron scattering results for Ce compounds.[22] The spin-relaxation rate for "magnetic ions," e.g., Tm and Nd, is of the Korringa-type at low T

and saturates to a constant value at high temperatures. This behavior has been found for TmSe (Ref. 22) and dilute Tm compounds.[23]

An inelastic peak was observed by neutron scattering in TmSe (Ref. 22) and in dilute Tm compounds.[23] Its origin can be either crystal-field splitting or the local charge excitation from the bonding to the antibonding mixed-valence state[24] with energy ΔE. The present approximations yield such an inelastic peak only if ΔE is very large. For small ΔE the effect is smeared by the linewidth of the f levels. Hence our model yields a more pronounced inelastic bump for Ce than for Tm.

The linewidth of the f levels is overestimated in both of our calculation methods. In the mode-mode coupling approach we neglected the vertex corrections which are expected to partially cancel the effect of the f-level self-energy, (3.5). In the Brillouin-Wigner approach we finally approximated the imaginary part of $M_{kJ_1}(z)$ with $(2J_1+1)\Gamma$, (4.16), which is expected to be frequency dependent and smaller than this value. $N(z)$ for large frequencies is not considerably affected by the above approximations, but $N''(\omega)$ for $|\omega| \lesssim \Delta E$ will be reduced and the inelastic peak is enhanced in this way.

The inelastic peak or strong deviations from a Lorentzian tail have not been observed for Ce. Such a peak should be present with an energy $\Delta E < 100$ meV for Ce in the valence range $3.5 < v < 3.8$. The nonexistence of the peak could be another indication that the valence of Ce is less than 3.5. In this case a Kondo-type singlet builds up, as can be seen from the Bethe ansatz solution of the impurity model,[30,31] and Ce compounds should be regarded as Kondo lattices.[37]

Note added in proof. An inelastic structure in the neutron scattering of dilute Ce in (La,Th) alloys has been reported by T. M. Holden, W.Y.L. Buyers, P. Martel, M. B. Maple, and M. Tovar, in *Valence Instabilities,* Ref. 3, p. 325. The origin of the rather broad structure, which disappears with temperature could be the bonding-antibonding transition.

ACKNOWLEDGMENTS

The author is indebted to D. Riegel, E. Holland-Moritz, and to the participants of the Centre Européen de Calcul Atomique et Moléculaire Workshop (Paris, 1983) for helpful discussions. The author acknowledges support as Heisenberg fellow by the Deutsche Forschungsgemeinschaft.

APPENDIX

Within the equation-of-motion method[11] we obtained the occupation numbers and the charge susceptibility via (3.11). The static spin susceptibility is not as straightforward since the self-energy $\Sigma(z)$ has to be evaluated in a small magnetic field. We write

$$\langle B_{JM}\rangle = \langle B_{JM}\rangle_{H=0} + \alpha_J MH, \quad \omega_{JM} = \omega_J^{H=0} + \gamma_J MH , \tag{A1}$$

and expand the expressions corresponding to (3.6) and (3.11) in an external field linearly in the field. Each equation has a linear term in $M_1 H$ and one in $M_2 H$, which lead to four equations to determine α_{J_1}, α_{J_2}, γ_{J_1}, and γ_{J_2}.

The self-energy $\Sigma(z)$ in a magnetic field depends on the operator $A_{M_1M_2}$. We obtain in second order in V,

$$\begin{aligned}\Sigma_{M_1M_2}(\omega) = -\frac{1}{2}\frac{(2J_2+1)\Gamma}{\langle B_{J_1M_1}\rangle + \langle B_{J_2M_2}\rangle} \\ \times\Bigg[\sum_{M_2',m}(M_2'm\,|\,M_1)^2\Bigg\{i(\langle B_{J_2M_2}\rangle + \langle B_{J_2M_2'}\rangle) \\ +(\langle B_{J_2M_2}\rangle - \langle B_{J_2M_2'}\rangle)\frac{2}{\pi}\left[\ln\frac{D}{2\pi T} - \psi\left[\frac{1}{2} - i\frac{\omega - E_{J_2M_2'} + E_{J_2M_2}}{2\pi T}\right]\right]\Bigg\} \\ +\sum_{M_1',m}(M_2m\,|\,M_1')^2\Bigg\{i(\langle B_{J_1M_1}\rangle + \langle B_{J_1M_1'}\rangle) \\ +(\langle B_{J_1M_1'}\rangle - \langle B_{J_1M_1}\rangle)\frac{2}{\pi}\left[\ln\frac{D}{2\pi T} - \psi\left[\frac{1}{2} - i\frac{\omega - E_{J_1M_1} + E_{J_1M_1'}}{2\pi T}\right]\right]\Bigg\}\Bigg] .\end{aligned} \tag{A2}$$

Owing to the magnetic field, $\Sigma_{M_1M_2}(\omega)$ is no longer a constant, but has an explicit frequency dependence. This modifies the sum over Matsubara poles that lead to (3.6) and (3.11). For $\Sigma_{M_1M_2}=\text{const}$, the sum just yields a digamma function, while for $H\neq 0$ it is summed over digamma functions. The expressions are complicated and the procedure is almost unpracticable.

In order to be consistent with the leading-order approximation the $\langle B_{JM}\rangle$ in (A2) should be the free-ion occupation numbers. Then the field-dependent terms of $\Sigma(\omega)$ are proportional to H/T, what gives rise to the Curie law at low T if the ground state is magnetic.

In the case of mixed-valence Ce the ground state is a singlet and the frequency dependence of $\Sigma(\omega)$ only gives

minor corrections[11] at low T and at high T. It is then justified to neglect the frequency dependence and use the following equations to determine χ_s^0:

$$\frac{\langle B_0\rangle-\langle B_{J_1M_1}\rangle}{\langle B_0\rangle+\langle B_{J_1M_1}\rangle}=\frac{2}{\pi}\mathrm{Im}\psi\left[\frac{1}{2}+\frac{\Gamma^*_{M_1}}{2\pi T}+i\frac{\Delta E_{M_1}}{2\pi T}\right] \tag{A3}$$

with

$$\Gamma^*_{M_1}=\Gamma/(\langle B_{J_1M_1}\rangle+\langle B_0\rangle)\,, \tag{A4}$$

$$\Delta E_{M_1}=E_{J_1M_1}+\omega_{J_1M_1}-E_0-\omega_0\,, \tag{A5}$$

$$\omega_{J_1M_1}=-\frac{\Gamma}{\pi}\left[\ln\frac{D}{2\pi T}-\mathrm{Re}\psi\left[\frac{1}{2}+\frac{\Gamma^*_{M_1}}{2\pi T}+i\frac{\Delta E_{M_1}}{2\pi T}\right]\right], \tag{A6}$$

and

$$\omega_0=\sum_{M_1}\omega_{J_1M_1}\,.$$

Equations (A3)—(A6) are used in Sec. V. The static susceptibility is obtained by numerical differentiation.

[1]Authors, in *Valence Instabilities and Related Narrow-Band Phenomena,* edited by R. D. Parks (Plenum, New York, 1977).

[2]Authors, in *Valence Fluctuations in Solids,* edited by L. M. Falicov, W. Hanke, and M. B. Maple (North-Holland, Amsterdam, 1981).

[3]Authors, in *Valence Instabilities,* edited by P. Wachter and H. Boppard, (North-Holland, Amsterdam, 1982).

[4]P. W. Anderson, Phys. Rev. 124, 41 (1961).

[5]A. Bringer and H. Lustfeld, Z. Phys. B 28, 213 (1977).

[6]T. V. Ramakrishnan, in *Valence Fluctuations in Solids,* Ref. 2, p. 13.

[7]N. Grewe and H. Keiter, Phys. Rev. B 24, 4420 (1981).

[8]T. V. Ramakrishnan and K. Sur, Phys. Rev. B 26, 1798 (1982).

[9]F. D. M. Haldane, Phys. Rev. Lett. 40, 416 (1978).

[10]J. H. Jefferson, J. Phys. C 10, 3589 (1977).

[11]P. Schlottmann, Phys. Rev. B 25, 2371 (1982); 26, 3474(E) (1982) (to be referred to as paper I).

[12]C. A. Balseiro and A. López, Solid State Commun. 17, 1241 (1975).

[13]M. E. Foglio, J. Phys. C 11, 4171 (1978).

[14]Y. Kuramoto, Z. Phys. B 37, 299 (1980).

[15]Y. Kuramoto and E. Müller-Hartmann, in *Valence Fluctuations in Solids,* Ref. 2, p. 139; E. Müller,-Hartmann, in *Electron Correlation and Magnetism in Narrow-Band Systems,* Proceedings of the Third Tanaguchi International Symposium, Mount Fuji, Japan, 1980, (Springer, Berlin, 1981), p. 178.

[16]W. Götze and P. Schlottmann, Solid State Commun. 13, 861 (1973).

[17]W. Götze and P. Schlottmann, J. Low Temp. Phys. 16, 87 (1974).

[18]P. Schlottmann, in *Valence Instabilities,* Ref. 3, p. 471.

[19]M. Luszik-Bhadra, H.-J. Barth, H.-J. Brocksch, G. Netz, D. Riegel, and H. Bertschad, Phys. Rev. Lett. 47, 274 (1981).

[20]D. Riegel, H.-J. Barth, M. Luszik-Bhadra, and G. Netz, in *Valence Instabilities,* Ref. 3, p. 497; H.-J. Barth, M. Luszik-Bhadra, and D. Riegel, Phys. Rev. Lett. 50, 608 (1983).

[21]D. Riegel (private communication).

[22]M. Löwenhaupt and E. Holland-Moritz, J. Appl. Phys. 50, 7456 (1979).

[23]E. Holland-Moritz, J. Magn. Magn. Mater. 38, 253 (1983).

[24]J. Mazzaferro, C. A. Balseiro, and B. Alascio, Phys. Rev. Lett. 47, 274 (1981).

[25]H. Mori, Prog. Theor. Phys. (Kyoto) 34, 399 (1965).

[26]R. Zwanzig, J. Chem. Phys. 33, 1338 (1960).

[27]W. Götze and K. H. Michel, in *Lattice Dynamics,* edited by A. A. Maradudin and G. K. Horton (North-Holland, Amsterdam, 1974), p. 500.

[28]P. Schlottmann, Phys. Status Solidi B 111, 161 (1982).

[29]M. E. Foglio and P. Schlottmann, Solid State Commun. 42, 423 (1982).

[30]P. Schlottmann, Z. Phys. B 49, 109 (1982).

[31]P. Schlottmann, Phys. Rev. Lett. 50, 1697 (1983); Z. Phys. B 51, 49 (1983).

[32]Note that Eq. (2.11a) of Ref. 11 should read $X_{m\sigma}=-\Delta\int(d\omega/\pi)f(\omega)G'_{m\sigma}(\omega)$ and Eq. (3.3a) should read $X_{m\sigma}=+(\Delta/\pi)(\langle B_0\rangle+\langle B_{m\sigma}\rangle)+\cdots$.

[33]G. Czycholl, H. Keiter, and E. Niebur, in *Valence Instabilities,* Ref. 3, p. 45.

[34]W. Götze and P. Wölfle, Phys. Rev. B 6, 1226 (1972).

[35]P. Schlottmann, J. Low Temp. Phys. 47, 27 (1982).

[36]P. Schlottmann, Phys. Rev. B 27, 558 (1983).

[37]J. W. Allen and R. M. Martin, Phys. Rev. Lett. 49, 1106 (1982).